

## Lattice dynamical models of adaptive spatio-temporal phenomena

SUDESHNA SINHA

The Institute of Mathematical Sciences, CIT Campus, Madras 600 113, India

**Abstract.** We describe the rich spectrum of spatio-temporal phenomena emerging from a class of models incorporating adaptive dynamics on a lattice of nonlinear (typically chaotic) elements. The investigation is based on extensive numerical simulations which reveal many novel dynamical phases, ranging from spatio-temporal fixed points and cycles of all orders, to parameter regimes displaying marked scaling properties (as manifest in distinct  $1/f$  spectral characteristics and power law distributions of spatial quantities).

**Keywords.** Spatio-temporal chaos; lattice dynamical models.

**PACS No.** 05.45

### 1. Introduction

A basic aim of modelling in physics is to provide suggestive conceptual frameworks for understanding complex phenomena, which are generic in physical systems. One seeks to construct simple yet effective models which are capable of capturing the essence of complicated dynamic processes as they occur in nature. For instance, one dimensional unimodal maps can serve as a versatile paradigm for low dimensional dissipative chaos, as they yield an extraordinarily rich spectrum of behaviours. From low dimensional nonlinear systems, which are now reasonably well understood, we reach out towards *nonlinear extended* systems. The hope is to build prototypes for such composite complex systems — prototypes which can yield a repertoire of dynamical behaviour reminiscent of well known behaviour in a wide range of fields where spatial extent is important, for instance turbulence, pattern formation (such as dislocation dynamics, intermittency in space-time, spatial patterns), Josephson junction arrays, neural dynamics, coupled systems of optically bistable devices, electron-hole plasmas and even parallel computing and evolutionary biology! [1]

So *complex systems research* has emerged as a field of vital importance in the last couple of decades, especially with the advent of high powered computing. It has had impact on several disciplines, as it investigates fundamental dynamic processes which occur in areas of physics, chemistry, and biology. This field of research involves the identification of dynamic processes and concepts which can be employed to understand large families of complex systems. It searches for principles of synthesis of dynamic processes at one level, which produce important dynamic phenomena at another collective level. Thus, in general terms, this field of research seeks to describe and

understand the origins of complex dynamic activities and to uncover the methods of modelling and possibly controlling various types of hierarchical dynamics.

One important prototype of extended complex systems is a nonlinear dynamical system with spatially distributed degrees of freedom, or alternately a spatial system composed of large numbers of low dimensional nonlinear systems. There are two principal variations of this scheme: first, the local dynamics can be simple and the interactions complicated in form; secondly, we can have complex local dynamics and simple mode of transmitting information between 'sites' (or 'degrees of freedom'). Here we will be concentrating on the latter situation where locally there is strong nonlinearity. The basic ingredients of such systems are: (i) creation of local chaos or local instability by a low dimensional mechanism and (ii) spatial transmission of energy and information by diffusion or transport (this interconnectivity can work as a global organizing principle in composite systems).

In principle spatio-temporal physics is completely described by the appropriate partial differential equations (PDE). Unfortunately, though, such equations are extremely difficult to solve, and practically intractable without simplifying assumptions and without employing distributed computing techniques. In order to follow complex systems dynamically over long times and over large spatial extents without resorting to heavy duty computing, physicists have used their imagination and evolved a hierarchy of models based on different discretization schemes. These computationally efficient schemes capture some of the essential physics of a very extensive range of natural phenomena. Two of the most successful schemes are cellular automata (CA) models where space, time and state variables are all discrete, and lattice dynamical systems (LDS) where space and time are discrete and state variables take continuous values. These models have led to the discovery of so many novel phenomena that they are now not merely the poor man's PDE, but bonafide models of complexity in space-time dynamics in their own right.

The aim of all these models is to capture in increasing degree the complexity inherent in nature and provide fitting descriptions of large interactive systems comprising of many elements. In particular, they address two widely occurring phenomena: *spatial fractality*, i.e., the spontaneous evolution of self similarity in space, and *low frequency noise* or  $1/f$  noise which represents the lack of a natural scale in time, therefore a kind of "fractality" in time. It is observed that many functional dependences, arising in a variety of experimental contexts, look like straight lines when plotted on a log-log scale, over a significantly large range. So these functions do not have natural length/time scales, that is, they are scale invariant or self similar. This is exemplified in space by spatial fractality, which is ubiquitous in nature, present as it is in spatial structures as diverse as mountain ranges, coastlines, clouds, colloidal aggregates, patterns of fracture, dielectric breakdown, porosity of soil and branching of roots [2]. In the temporal regime, we have  $1/f$  noise:  $S(f) \sim 1/f$ , where  $f$  is the frequency and  $S(f)$  is the power. (This is also known as "flicker noise" in astronomy, in the context of light from quasars for instance [3]). Such "noise" (or from some viewpoint "signal") is characterized by variations on all timescales, and appears in events as varied as resistance fluctuations, sand flow in an hourglass and even traffic and stock market movements [3]. The generality and ubiquity of these two phenomena have puzzled scientists for a long time. The study of fractality, though, is mostly confined to the level of characterization (for example plotting results of experiments on log-log scales and associating the slope with some kind of fractal

dimension). What theorists would really like to do of course, is to find the *dynamical origin* of these phenomena. So, the success of many of the models suggested should be judged with respect to their ability to *dynamically yield space-time fractality*.

In this article we will focus on a class of complex networks, proposed very recently by Sinha and Biswas [4]. These models incorporate adaptive dynamics on a lattice of nonlinear (typically chaotic) elements, and are relevant as prototypes for complex nonlinear self regulatory processes in physics and biology. We will describe the wealth of spatiotemporal structures these models yield, and characterize their “phases” and scaling patterns.

## 2. Model

Here we describe the essentials of the proposed class of models, which falls under the general category of lattice dynamical systems. First, we focus on the *one dimensional unidirectional* model where time is discrete, labelled by  $n$ , space is discrete, labelled by  $i$ ,  $i = 1, N$ , where  $N$  is system size, and the state variable  $x_n(i)$  (which in physical systems could be quantities like energy, velocity, pressure or concentration) is continuous. Each individual site in the lattice evolves under a suitable nonlinear map  $f(x)$ . For instance, the local map  $f(x)$  can be chosen to be the logistic map, which has widespread relevance as a prototype of low-dimensional chaos, i.e.

$$f(x) = 1 - ax^2,$$

$x \in [-1.0, 1.0]$ , with the nonlinearity parameter  $a$  chosen in the chaotic regime, for instance  $a = 2.0$  in all numerical experiments in [4]. Another possible choice in the local dynamics is the circle map which is relevant in systems involving nonlinear oscillatory behaviour [6, 7]. This is given by

$$f(x) = x - \frac{\kappa}{2\pi} \sin(2\pi x)$$

with  $\kappa$  determining the strength of the nonlinearity.

Now, on this nonlinear lattice a self regulatory threshold dynamics is incorporated. The adaptive mechanism is triggered when a site in the lattice exceeds the critical value  $x_c$  i.e., when a certain site  $x_n(i) > x_c$ . The supercritical site then relaxes (or “topples”) by transporting its excess  $\delta x = (x_n(i) - x_c)$  to its neighbour as follows:

$$\begin{aligned} x_n(i) &\rightarrow x_c \\ x_n(i+1) &\rightarrow x_n(i+1) + \delta x. \end{aligned} \tag{1}$$

This algorithm thus induces a unidirectional nonlinear transport down the array (by initiating a domino effect). The boundary is open so that the “excess” may be transported out of the system. Note that the adaptive (“toppling”) mechanism in the model is locally conservative, whereas the intrinsic dynamics of the elements is dissipative. This kind of threshold mechanism imposed on local chaos, makes the above scenario especially relevant for certain mechanical systems like chains of nonlinear springs, as also for some biological systems, such as synapses of nerve tissue (note that individual neurons display complex chaotic behaviour and have step function-like responses to stimuli).

The threshold adaptive dynamics is reminiscent of the Bak–Tang–Wiesenfeld CA algorithm [8], or the “sandpile” model, which gives rise to self organized criticality (SOC). This model is however significantly different, the most important difference being that the self regulatory mechanism now occurs on a nonlinear “substrate”, i.e. there is an “intrinsic” or “internal” deterministic dynamics at each site. Further, the state variable analogous to the integer “height” variable  $z$  in the sandpile model is continuous here. All this accounts for enhanced complexity and this system is thus capable of exhibiting a wider repertoire of dynamics. So, unlike 1D-SOC, the one dimensional model here is not trivial and can give rise to many interesting features, including a host of dynamical phases.

The dynamics depends on the algorithm for autonomously updating each site and propagating threshold coupling between sites. The first possible case is one where these two evolutionary steps are carried out separately. Here the system is allowed to relax completely before each chaotic update. One self-regulatory update of all existing supercritical sites in the lattice, performed according to (1) constitutes one relaxation time step. This relaxation step may in turn create some other supercritical sites. After  $\Delta$  such relaxation steps, the system undergoes the next chaotic update. In some sense then, time  $n$  associated with the chaotic dynamics is measured in units of  $\Delta$ . When  $\Delta$  is large enough ( $\Delta \gtrsim O(N)$ ) as in [4], the adaptive dynamics begins after each step in the site dynamics and continues till the system has reached a steady state where all sites are less than critical, i.e. all  $x(i) \leq x_c$ , and the system is stationary, after which the next step in the site dynamics takes place. So the time scales of the two dynamics, the intrinsic chaotic dynamics of each lattice site and the adaptive relaxation, are adiabatically separable. The relaxation mechanism is much faster than the chaotic evolution, and this enables the system to relax completely before the next chaotic iteration. The complete dynamical picture then is as follows: after every time step in the chaotic evolution,  $n$ , the system undergoes a self regulatory relaxation leading to stable “under-critical” configurations  $\{x_n(i)\}$ , after which the next chaotic iteration of the lattice takes place, governed by the nonlinear evolution mapping:  $x_{n+1}(i) = f(x_n(i))$ . One can also consider the local chaos in the maps to be an “intrinsic” or “internal” perturbation (as opposed to “external” perturbation in the “sandpile” model, which is effected by dropping “sand” from outside). In this sense then, the system above (as its allowed to relax fully between chaotic updates) operates in the “dilute” perturbation limit.

A random driving force can also be introduced in the model. Under this, the system is perturbed at some site  $j$  in the lattice:  $x_n(j) \rightarrow x_n(j) + \sigma$  where  $\sigma$  is the strength of the perturbation and  $j$  is chosen at random. The spatial extent of the perturbation can be gauged by the number of such random sites affected at any given update (which we denote by  $N_r$ ). The random driving force is operative at time scales comparable to the chaotic dynamics. When this is much slower than the adaptive dynamics, as in [4], the scenario is similar to the SOC algorithm, where the driving force (perturbation) is very dilute, and the system is allowed to relax completely before the next perturbation and time is usually measured in units of the perturbing force (for example, in units of grains of “sand” added in the sandpile model of SOC) and the configurations studied are the relaxed configurations after each perturbation step. This is quite different from the coupled map lattice (CML) dynamics [9], where the coupling is incorporated in the map evolution step.

At the other end of the spectrum is the limit of very small  $\Delta$ —which is practically analogous to CML. Here the local nonlinear dynamics and chaotic updates take place almost simultaneously. It is evident that lowering  $\Delta$  essentially allows us to move from a picture of adiabatically separated adaptive processes to one where adaptive processes overlap, and disturbances do not die before the subsequent chaotic update, i.e. *the tails of the relaxation processes carry over to the next event and there are “interference” effects.* The effect of relaxation time on dynamical characteristics was investigated in detail in [7].

The relevant parameters in the model are the local nonlinearity parameter, (for instance,  $a$  in the case of logistic maps, and  $\kappa$  in the case of circle maps), strength of perturbation,  $\sigma$  and the relaxation time  $\Delta$ . The simulations are done with random initial conditions for the  $x(i)$  and all transients are allowed to die. Two of the most interesting features to be examined are (i) the temporal evolution of local quantities, such as the individual sites  $x_n(i)$ , and (ii) the temporal evolution of globally defined quantities, such as “avalanches”, which are defined as the total number of “active” sites, i.e. sites that have “toppled” during the adaptive relaxation, denoted by  $s$ . The spatial aspects of interest are the distribution of  $x(i)$  and the presence of clustering and coherence in space as indicated by the cluster distribution at any point in time (or snapshot). Besides these generic spatio-temporal measures, some other quantities may be of interest in certain contexts. For instance, the dynamics and distribution of the “drop rate”, i.e. the “excess” transported out of the lattice edge during relaxation, may be significant in some physical situations (such as in phenomena reminiscent of the “dripping faucet” scenario).

Note that  $x_c$  is the most significant parameter in the system. For instance, for the case of the local logistic map ( $f(x) = 1 - 2x^2$ ), where  $-1.0 < x_c < 1.0$ , numerical simulations show the presence of the many “phases” in  $x_c$  space [4]. For example, for  $x_c \leq 0.5$  the dynamics goes to a fixed point. When  $0.5 < x_c < 1.0$ , the dynamics is attracted to *cycles* whose periodicities depend on the value of  $x_c$ . By tuning  $x_c$  one thus obtains cycles of varying orders. So in a sense, this model (by variation of a single parameter) provides a wide repertoire of dynamics for lattice dynamical systems, just as the logistic map does for one dimensional systems (by variation of the nonlinearity parameter). Thus it may be used as a paradigm for complex behaviour in extended systems.

Note another important feature here. If the same adaptive dynamics was imposed on a random lattice, that is a bunch of noisy elements, we would not have recovered any of the above mentioned phases. For these phases to occur we crucially require a *deterministic dynamics*, even if entirely chaotic. *The difference between stochastic noise and deterministic chaos is of vital importance here.*

We can also introduce the bidirectional model. This is given by the following algorithm: if  $x_n(i) > x_c$ , the supercritical site then relaxes to  $x_c$  by transporting the excess  $(x_n(i) - x_c)$  equally to its two neighbours:

$$\begin{aligned} x_n(i) &\rightarrow x_c \\ x_n(i+1) &\rightarrow x_n(i+1) + \delta x \\ x_n(i-1) &\rightarrow x_n(i-1) + \delta x \end{aligned} \tag{2}$$

where  $\delta x = (x_n(i) - x_c)/2$ . Now disturbances in the course of self-regulation, can spread like “ripples” and “refract”. The dynamics of the bidirectional model looks, by and

large, like a “fuzzier” or “noisier” version of its unidirectional counterpart. The details will be discussed in the following sections.

Before we move on to a specific example in §3, we will write down the generalized model in  $d$  dimensions with  $m$  state variables. Let each state variable defined at a certain site in the lattice be denoted as  $x^j(\mathbf{i})$ , where  $\mathbf{i}$  is a  $d$  dimensional vector representing the coordinates of the site in the  $d$  dimensional lattice, and  $j$  represents a particular state variable, taking values from 1 to  $m$ . If a certain state variable, say  $x^j(\mathbf{i})$  at a certain site  $\mathbf{i}$  in the  $d$  lattice exceeds the critical value,  $x_c^j$ , then the excess is transported equally to its neighbours. (Note that in general we may have different critical values for different state variables, and these are given by  $m$  numbers,  $x_c^j, j = 1, 2, \dots, m$ ). Also note that in  $d$  dimensions the number of neighbours (assuming isotropic transport) is  $2d$ . Given these the adaptive dynamics then is

$$\begin{aligned} x_n^j(\mathbf{i}) &\rightarrow x_c^j \\ x_n^j(\mathbf{i} + \boldsymbol{\delta}) &\rightarrow x_n^j(\mathbf{i} + \boldsymbol{\delta}) + \delta x, \end{aligned} \quad (3)$$

where the quantity  $\delta x$  gives the excess, which is equally distributed among the  $2d$  neighbours:  $\delta x = (x^j(\mathbf{i}) - x_c^j)/2d$ . The vector  $\boldsymbol{\delta}$  is  $d$ -dimensional, comprising of only one nonzero element ( $= 1$  or  $-1$ ) and it gives the coordinates of the nearest neighbours of the critical site to which the excess is transported.

Some other variations to the model are also possible. For instance, we can investigate the effect of changing boundary conditions. In particular, we can incorporate the adaptive dynamics on a lattice with periodic boundary conditions, that is on a ring of nonlinear elements. Further, for instance, one can implement the adaptive dynamics (or transport) on a hierarchical lattice, in order to evoke scaling phenomena reminiscent of energy cascade in turbulent media. In general then, several variations of this class of models can be invoked in order to tailor the generalities to suit the specific physics at hand and account for particular phenomena.

In this article we will focus on one representative example, namely, adaptive dynamics on logistic maps. We give a detailed description of the system and its emergent phenomena in the section below.

### 3. Adaptive dynamics on logistic maps

In this model the local on-site dynamics is given by logistic maps. The specific form of the logistic map used (without any loss of generality) is:  $f(x) = 1 - ax^2, x \in [-1, 1]$ , operating in the chaotic regime, i.e.,  $a = 2$ . We deal with the case of  $\Delta$  large, which allows complete relaxation of the active sites before the subsequent chaotic update. First, we describe the unidirectional case, with and without external noise, and then describe the bidirectional model.

#### 3.1 Unidirectional model: Phenomenology

As noted in §2, the most significant parameter in the system is the critical  $x_c$  ( $x_c \in (-1, 1)$ ), and by tuning  $x_c$  one obtains the following phases: The first phase is the

### Adaptive spatio-temporal phenomena

fixed point region which occurs when  $x_c < 0.5$ . Here the system goes to a coherent state where all sites  $x_n(i) = x_c$  for all times (after a short transience). This spatiotemporal invariance is achieved for all perturbation strengths and system sizes. The size of the avalanches is always equal to  $N(N + 1)/2$  and the duration of the avalanches equal to  $N$  [4]. In this parameter regime, then, the adaptive mechanism suppresses the underlying chaos in the lattice and yields spatiotemporal regularity.

The model (in the range  $x_c < 0.5$ ) may then be considered as a tool for “controlling” [10] an ensemble of chaotic elements, as it can very effectively force the system to a temporally invariant and spatially coherent state:  $x_n(i) = x_c, i = 1, \dots, N$  for all  $n$ . Note that this spatiotemporal control is robust with respect to system size and perturbation strengths. Couched in the language of control theory, we can consider  $x_c$  to be the “desired state” of the system [10]. The “error signal” is then determined by the difference between the existing state and the desired state. A positive error signal triggers off the self regulatory feedback mechanism which drives the system to adaptively control its dynamics back to the desired state (when the error is zero).

When  $x_c = 0.5$  we still have a coherent state with all  $x(i) = x_c$ . When there is no noise the avalanches are of size zero as there are never any active sites in the lattice, as  $x = 0.5$  is a fixed point of the map  $f(x)$ . Under a random driving force ( $N_r \neq 0$  and  $\sigma \neq 0$ ) the

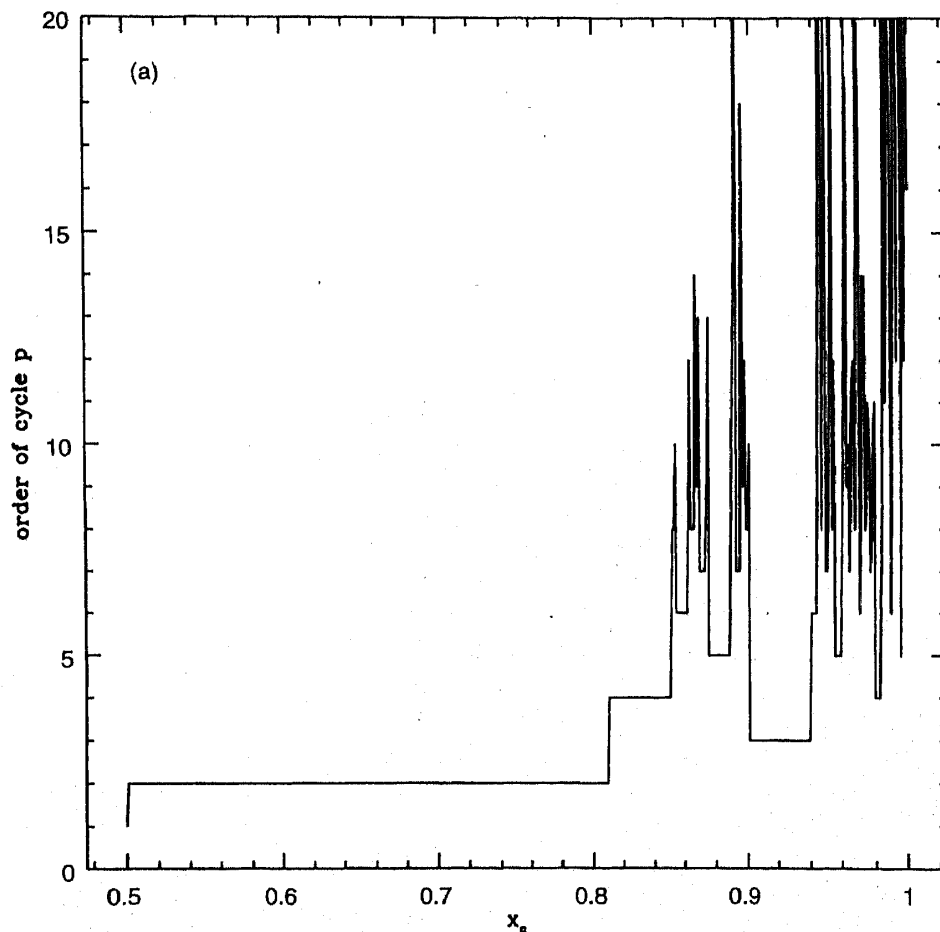
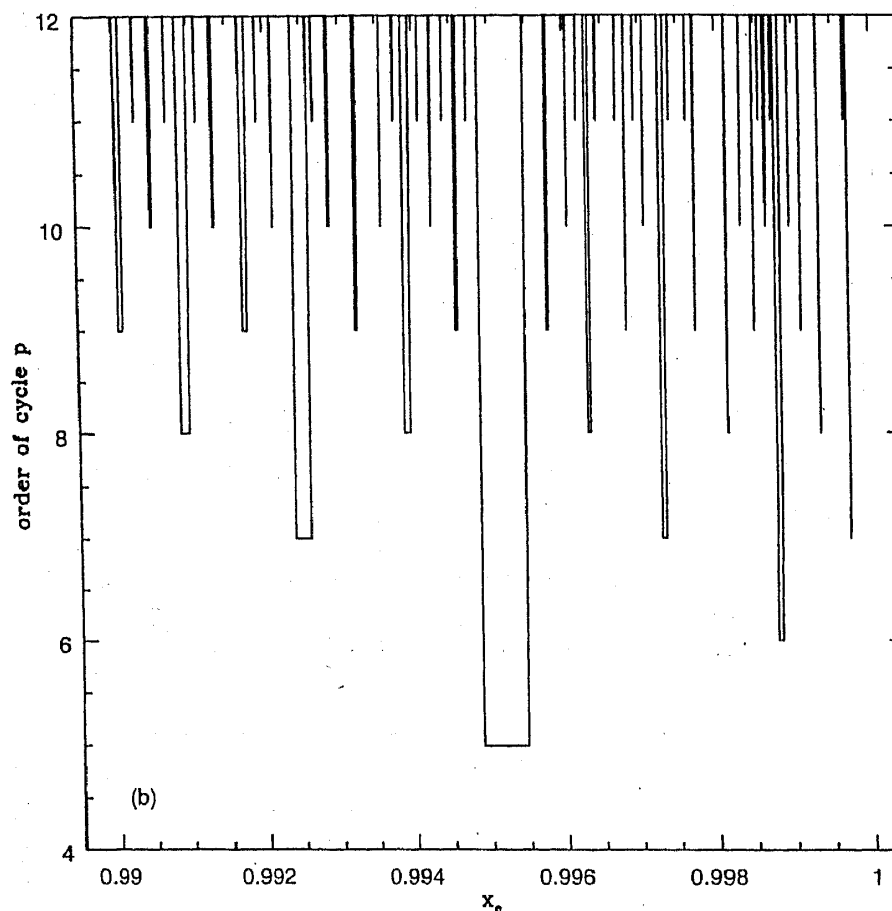


Figure 1a. (Continued)



**Figure 1.** Order  $p$  of the cycle obtained at various values of the parameter  $x_c$ , in a unidirectional adaptive model on a lattice of logistic maps ( $\sigma = 0$ ), depicted for the ranges: (a)  $x_c \in [0.5, 1.0]$  ( $k$  up to 20 is shown) and (b)  $x_c \in [0.99, 0.9999]$  ( $k$  up to 12 is shown).

avalanches are triggered off, and they have a random distribution of sizes, as the avalanche size is simply determined by the distances of the perturbed sites from the edge of the lattice, and from each other, and these are statistically random quantities.

When  $0.5 < x_c < 1.0$ , the temporal evolution of the lattice sites (and avalanches) is attracted to a cycle whose periodicity (order)  $p$  depends on  $x_c$  [4]. For example, by tuning  $x_c$  one obtains the following dynamical phases: for  $0.5 < x_c \leq 0.809\dots$ , we get 2-cycles, for  $0.809\dots < x_c < 0.85$  we get 4-cycles, for  $x_c \sim 0.86$  we get 6-cycles, for  $x_c \sim 0.88$  we get 7-cycles, for  $x_c \sim 0.9$  we get 10-cycles and for  $x_c \sim 0.98$  we get 4-cycles, and so forth. When there is no external perturbing force ( $\sigma = 0$ ) these cycles are *exact*. From figure 1 (which gives the order of the cycle,  $p$ , supported at various values of  $x_c$ ) it is clearly evident that the system yields a rich repertoire of cyclic patterns. Note here that it is possible to obtain a detailed and rigorous analytical picture of the spatial and temporal characteristics of the various cycles: see [5]. This analysis [5] provides a dynamical basis for the various phases found in this model. Further, the analysis also gives exact scaling relations for the position and width of periodic windows in  $x_c$  space. Due to constraints of space, however, we will not touch upon those analytical results in this article, but concentrate instead on the numerical results found principally in [4].



## Adaptive spatio-temporal phenomena

Temporally, then, we obtain cycles of varying orders. Now, spatially, we would like to discern the degree of “coherence” in the spatial profile at any instant of time (or snapshot) by examining the spatial patterns in  $x_n(i)$ ,  $i = 1, 2, \dots, N$ . For instance, we can quantify spatial clustering in the landscape by defining the size  $c$  of a spatial cluster as the number of consecutive sites for which the inequality  $|x_n(i+1) - x_n(i)| < \epsilon$  holds, where  $\epsilon$  is a small number. (The results are not very sensitive on the choice of  $\epsilon$ ). Very large cluster sizes, i.e.  $c \sim O(N)$ , indicate a smooth, almost coherent, profile, whereas profiles with maximum cluster size  $c_{\max} \sim 10$  reflects a rough profile.

It is observed that for values of  $x_c$  supporting low order periodicities, there often exists one very large cluster. In addition to this large (isolated) cluster, there exist many smaller clusters which are distributed approximately as a power law. For instance, for the case of  $x_c = 0.98$  which supports a 4-cycle, we usually find one large cluster,  $c_{\max} \sim N/2$ , and a host of smaller clusters (see figure 2). The coarse grained distribution of the small cluster sizes,  $P(c)$ , appears to be a power law:  $P(c) \sim c^{-\phi_c}$ , with exponent  $\phi_c$  depending on the specifics of the model [11]. On addition of noise the spatial profile gets more uneven, as the clusters break into smaller clusters. For instance, for  $x_c = 0.98$ ,  $\sigma = 0.2$ ,  $c_{\max} \sim N/4$ , that is the largest cluster is around half as large as in the  $\sigma = 0$  case.

For larger  $x_c$  supporting cycles of high order (for example,  $x_c = 0.99$ ) we find that the landscape consists of several small clusters of size  $c$ , occurring over a range of scales,

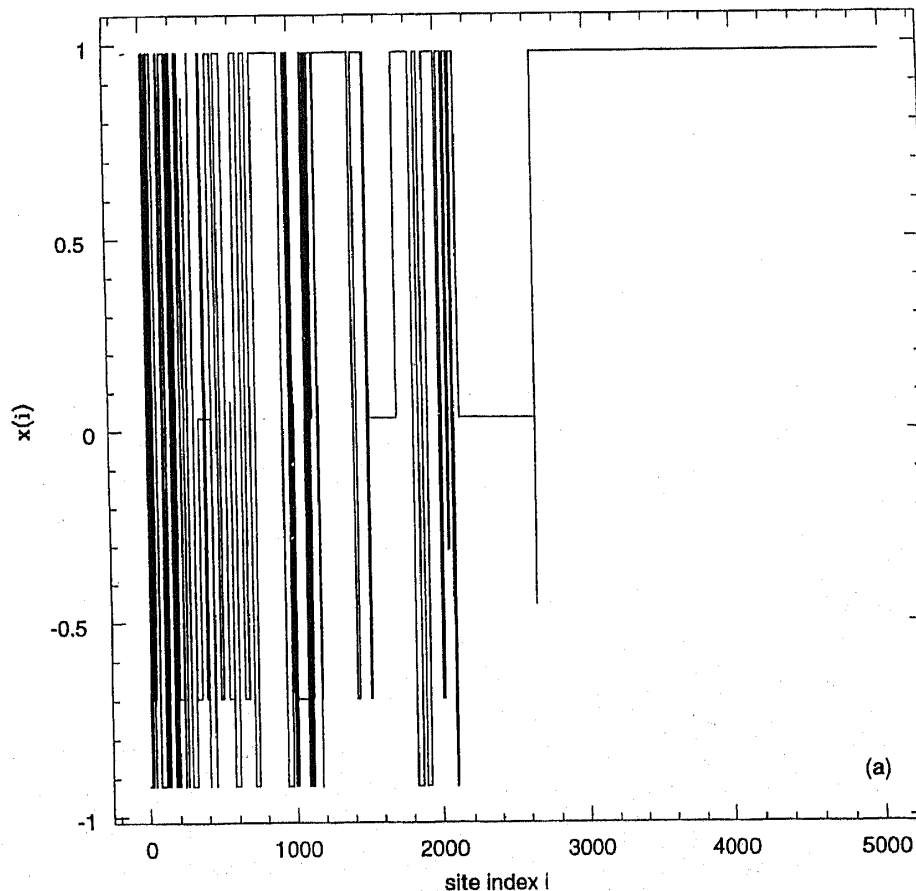
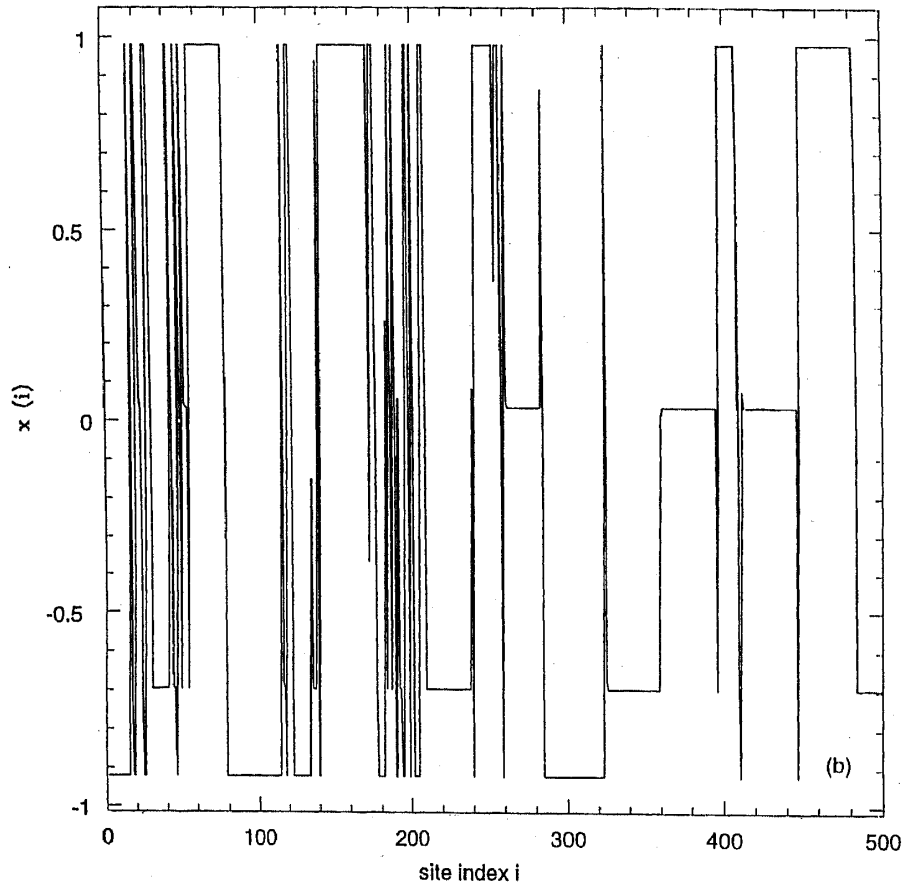


Figure 2a.



**Figure 2.** A plot of state variable  $x(i)$  vs site index  $i$ , in a unidirectional adaptive model on a lattice of logistic maps, at  $x_c = 0.98$ ,  $\sigma = 0$ , for a lattice of size  $N = 5000$ . In (a) we depict the entire lattice:  $i = 1, \dots, 5000$ . Note the existence of one very large cluster (all sites with  $2648 \leq i \leq 5000$  have  $x(i) = 0.98$ ). In (b) we depict a blown up version of the section of the lattice with  $1 \leq i \leq 500$ . Note the range of cluster sizes.

up to  $c_{\max} \sim 10$ . The profile is now very rough (see figure 3). Also, note that the addition of noise now does not appreciably alter the picture. The distribution  $P(c)$  follows a power law:  $P(c) \sim c^{-\phi_c}$ , where the exponent  $\phi_c$  depends on the particulars of the model.

### 3.2 Unidirectional dynamics under weak noise

Very interesting phenomena emerge on the addition of weak noise. When noise is very weak (i.e.,  $\sigma$  is small, and number of affected sites,  $N_r$  is small, say  $N_r/N < 0.1$ ) then the dynamics remains regular, especially for low  $x_c$  values supporting low order cycles. On adding moderate noise,  $\sigma \sim 0.01$ , and  $N_r/N \sim 0.1$ , we get interesting results for certain  $x_c$  values: namely large  $x_c$  with a reasonably wide window of low periodicity associated with it. At these parameters the system yields a well defined  $1/f$  spectrum:  $S(f) \sim 1/f^\phi$ ,  $\phi \sim 1.0$ . So the time profile now has variations on all scales, with interesting “cyclic” looking broad trends. Figure 4 displays a representative example of  $x_c = 0.98$ ,  $\sigma = 0.01$ ,  $N_r = 1$  and  $N = 20$  which yields a power spectrum with  $\phi \sim 0.93 \pm 0.06$ . Also notice

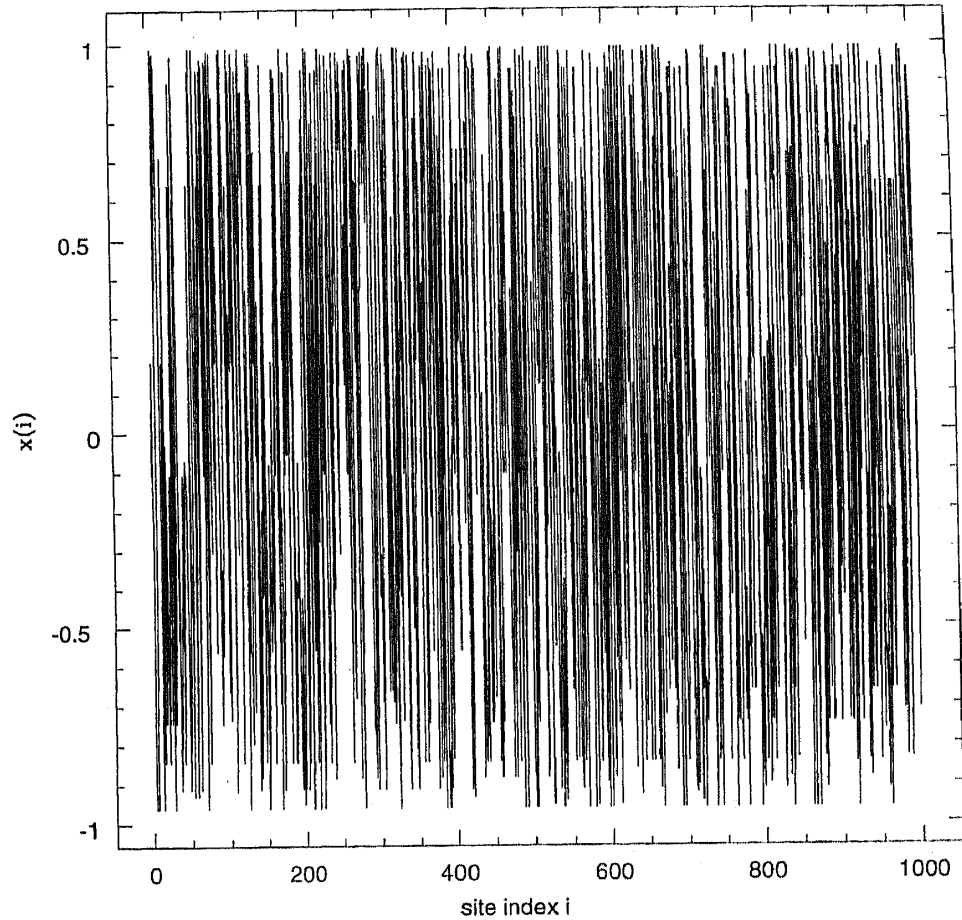


**Figure 3.** A plot of state variable  $x(i)$  vs site index  $i$ , in a unidirectional adaptive model on a lattice of logistic maps, at  $x_c = 0.99$ ,  $\sigma = 0$ , for a lattice of size  $N = 1000$ . Note the rough looking profile.

that there is a large peak in the spectrum at  $f = \frac{1}{4}$ , which is the period associated with  $x_c$  when  $\sigma \sim 0$ .

This kind of temporal scale invariance is reflected in the distribution of avalanche size  $s$ , which falls as a power law:  $P(s) \sim s^{-\phi_s}$ . It is also observed that  $P(s)$  is considerably peaked at large values of  $s$  ( $s \sim O(N)$ ). This hump at large  $s$  reflects the very large events, which occur approximately periodically, with the period given by the  $\sigma = 0$  model. Figure 5 gives the  $P(s)$  vs  $s$  curve for the representative case of  $x_c = 0.9$ . The exact value of the exponent  $\phi_s$  depends on the system parameters, and usually has values close to 1.0 (here for  $x_c = 0.9$ ,  $\phi_s \sim 1.2 \pm 0.2$ ).

A further quantity of interest would be the sizes of active clusters,  $k$ , at any given instant of time (or snapshot) after the relaxation has taken place. This is determined by the number of consecutive sites that move (or become active) during the course of an adaptive process. This number can vary from 1 to  $N$ .

Numerical experiments indicate that the distribution  $P(k)$  follows a power law:  $P(k) \sim k^{-\phi_k}$ . The exponent  $\phi_k$  depends on the particulars of the system and varies in the range  $\sim 1.0$  to  $2.0$ . For instance, from figure 6 (which shows a representative example of  $x_c = 0.88$ , with  $P(k)$  obtained by averaging over  $2 \times 10^4$  realizations) it is clearly evident

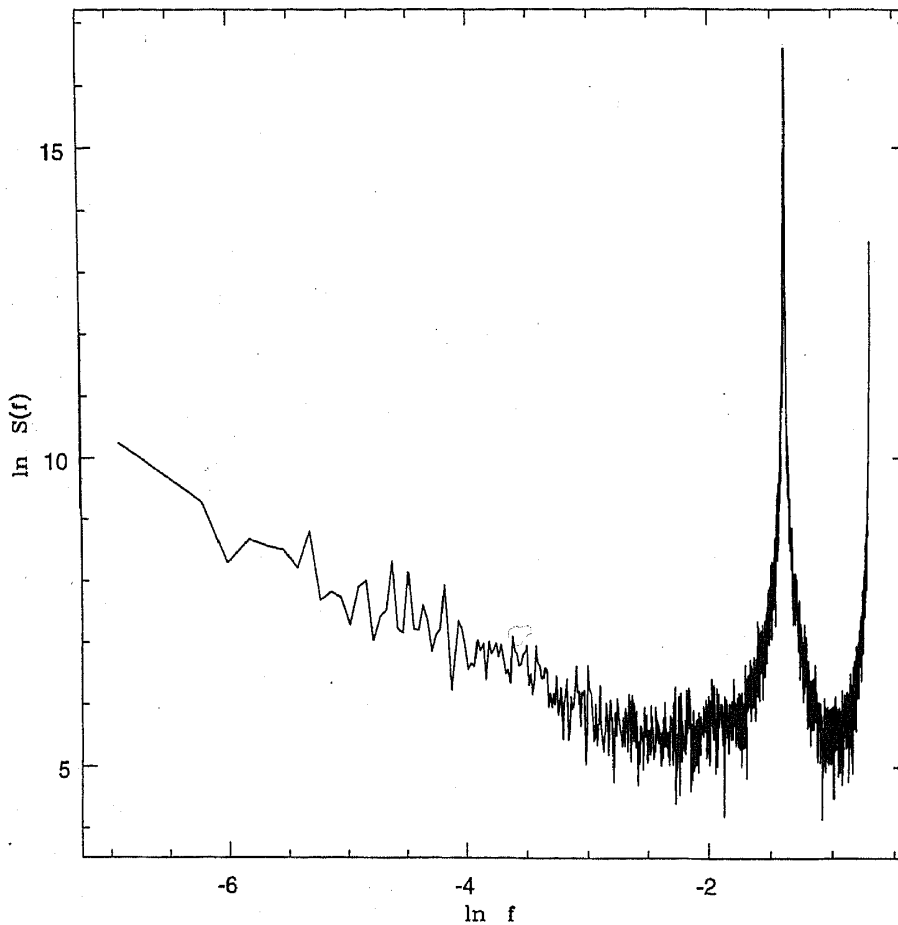


**Figure 4.** Power spectrum of avalanches in a unidirectional adaptive model on a lattice of logistic maps, with  $x_c = 0.98$ ,  $\sigma = 0.01$ , and  $N_r = 1$ ,  $N = 20$ . We have averaged over 8 time runs of 2048 each. The abscissa has  $\ln f$ , where  $f$  is the frequency ( $f \in (0, 0.5]$ ), and the ordinate has  $\ln S(f)$ , where  $S(f)$  is the power.

that there exists well defined scaling, with the exponent  $\phi_k \sim 1.1$ . This scaling reflects the fact that responses to perturbation (or energy dissipation) in this model takes place over a range of length scales, starting from small local rearrangements to large events where the transport activity is at a wider scale involving all the elements of the lattice.

For large values of  $x_c$  supporting very high order cycles, the spectra is noisy and flat ( $S(f) \sim 1/f^0$ ) even for very weak noise. Also, the distribution of avalanche size  $s$  is a gaussian. So the system now behaves more like a bunch of random elements.

### 3.3 Bidirectional model: Phenomenology

Bidirectional transport mimics its unidirectional counterpart closely, but seems to be a noisier or “fuzzier” version of it. Thus we find that for  $x_c \leq 0.5$  all the sites are randomly distributed with a small deviation around the mean which is almost equal to  $x_c$ . The avalanches are all of the maximum possible size  $s_{\max} = \Delta \times N$ . When  $0.5 < x_c \lesssim 0.8$  the sites get attracted to noisy 2-cycles, as is evident through the power spectrum of the

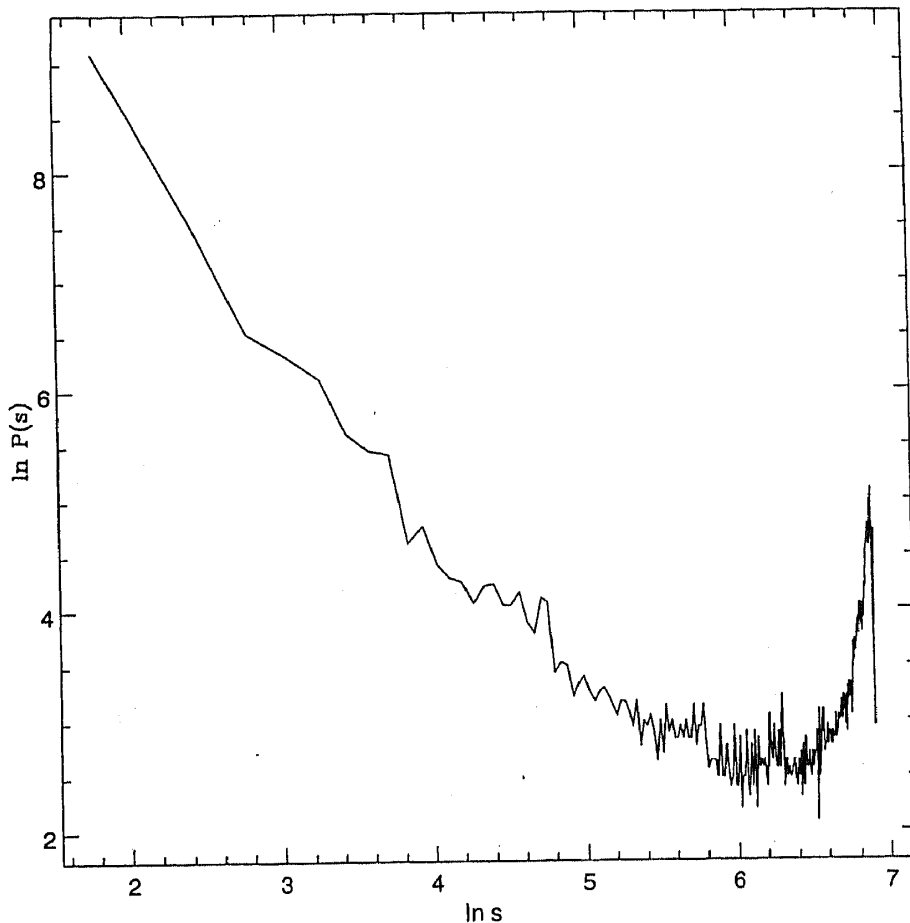


**Figure 5.** Plot of the distribution of avalanche sizes:  $\ln P(s)$  vs  $\ln s$ , in a unidirectional adaptive model on a lattice of logistic maps, for  $N = 1000$ ,  $x_c = 0.9$ , and  $\sigma = 0.1$ . We sample  $2 \times 10^4$  configurations.

temporal evolution of the individual sites which exhibit a large (but not clean) peak at  $1/2$ . The avalanches evolve as exact 2 cycles, alternating between 0 and  $s_{\max}$ . Further, as we tune  $x_c$  we obtain a noisy 4-cycle, and so forth.

As  $x_c$  gets larger we have a rather complex scenario with a host of scaling properties emerging in space and time. Firstly, for certain  $x_c$  values, namely large  $x_c$  with a reasonably wide window of low periodicity associated with it, we observe a time profile having variations over a wide range of scales, giving rise to a well defined  $1/f$  spectrum. For instance, in the example shown in figure 7, the system ( $x_c = 0.98$ ) displays a prominent low frequency spectrum, with  $\phi \sim 1.54 \pm 0.06$ . Note also, the existence of a sharp peak at  $f = \frac{1}{4}$ , which is the frequency of the exact cycle associated with the unidirectional  $\sigma = 0$  system. (It is then evident from comparing figures 4 and 7, that the spectrum for the bidirectional model is strikingly similar to that obtained from unidirectional dynamics under weak noise).

The active clusters, typically, now come in all sizes, indicating again that activity is taking place on several scales, starting from small rearrangements to large events sweeping through the lattice. The distribution of active cluster sizes  $P(k)$ , displays a clearly defined power law:  $P(k) \sim k^{-\phi_k}$ . The exponent depends on the particular system

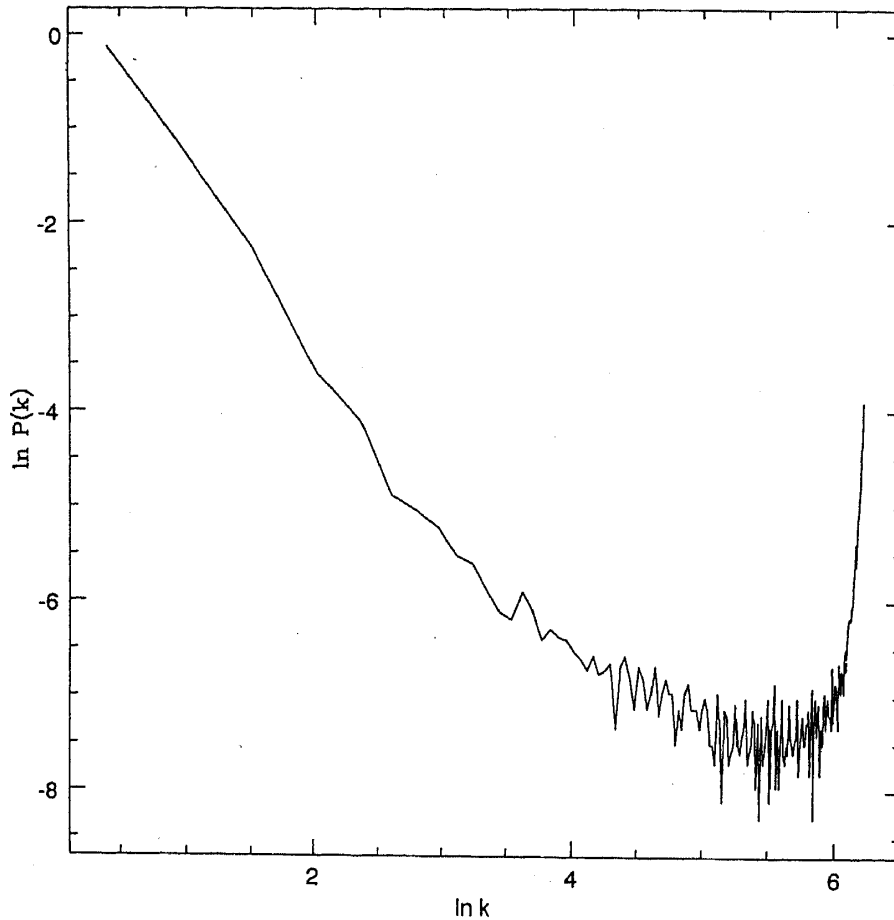


**Figure 6.** Plot of the distribution of active clusters:  $\ln P(k)$  vs  $\ln k$ , in a unidirectional adaptive model on a lattice of logistic maps, for  $x_c = 0.88$ ,  $\sigma = 0.2$ ,  $N = 500$ . We have averaged over  $2 \times 10^4$  configurations. Notice the enhanced probability of finding large active clusters, as evident from the rising  $P(k)$  around  $k_{\max} \sim N/5$ .

we examine. For instance, for  $x_c = 0.9$  and  $\sigma$  in the range 0.0 to 0.2, we obtain  $\phi_k \sim 4.0$ , and for  $x_c = 0.98$ , for noise levels  $\sigma = 0.0$  to 0.2, we obtain  $\phi_k \sim 2.0$ . This scaling reflects the fact that responses to perturbation (or energy dissipation) in this model takes place over a range of length scales.

A further quantity of interest would again be the distribution of avalanches. Here we focus only on the coarse grained distribution, as the range of values of  $s$ , from 0 to  $s_{\max} = \Delta \times N$ , is rather large. First, it is observed that there is a considerable hump at large values of  $s$  ( $s \rightarrow s_{\max}$ ). This is related to the fact that there are large events which occur approximately periodically (with the same period as that of the system's unidirectional counterpart). For instance, for  $x_c = 0.98$ , approximately one in every four avalanches is very large. (Such avalanches actually take infinitely long to settle down, and so their size is bound only by finite  $\Delta$ , i.e.  $s = s_{\max} = \Delta \times N$ .) For small sizes, it was found that the distribution falls as a power law:  $P(s) \sim s^{-\phi_s}$ . While this power-law trend persists for weak noise, under addition of moderate noise the system often yields an exponentially falling distribution:  $P(s) \sim e^{-\phi_s s}$ . Further, very high  $x_c$  ( $x_c \rightarrow 1.0$ ) also yields such exponentially decaying  $P(s)$ .

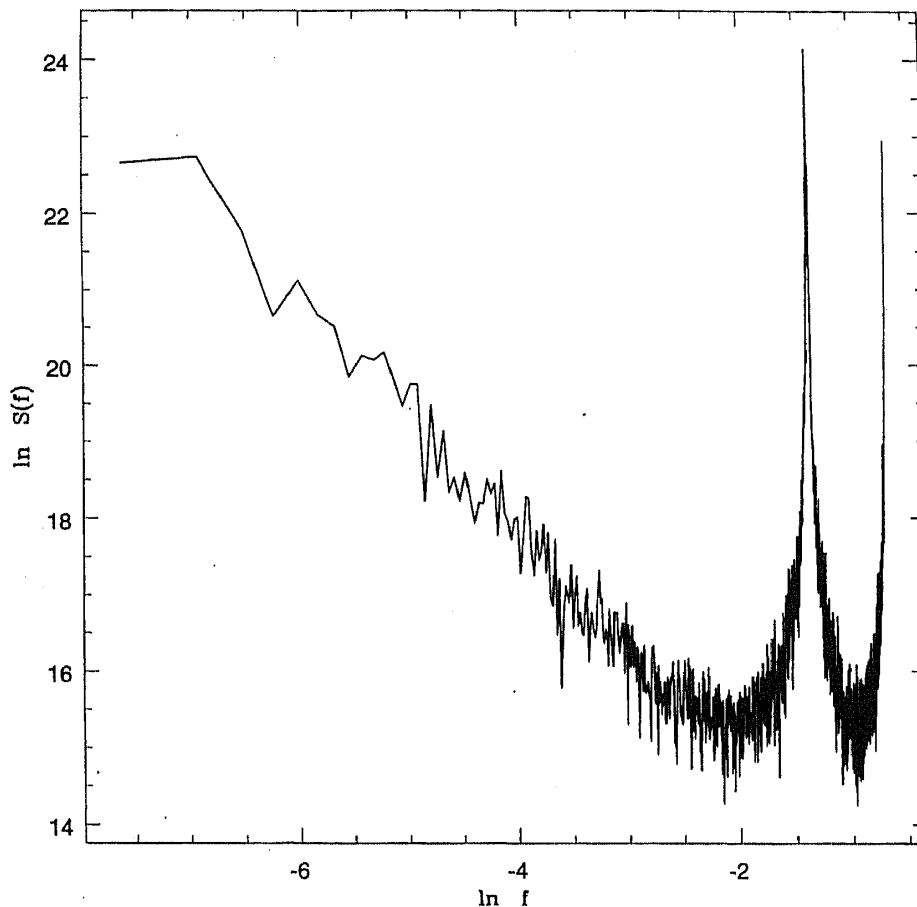


**Figure 7.** Power spectrum of avalanches in a bidirectional adaptive model on a lattice of logistic maps, for  $x_c = 0.98$ ,  $N = 20$ , and  $\sigma = 0.01$ ,  $N_r = 3$ . We average over 8 time runs of 2048 each. The abscissa has  $\ln f$ , where  $f$  is frequency ( $f \in (0, 0.5]$ ), and the ordinate has  $\ln S(f)$ , where  $S(f)$  is the power.

Spatially, we obtain power law-like distributions for spatial cluster sizes  $c$ . We find a host of small clusters up to a size of  $c_{\max} \sim N/25$ . Note that the addition of noise does not appreciably alter the roughness of the profile. Note, also, that unlike its unidirectional counterpart, there are no large clusters here. The coarse grained distribution of the small cluster sizes  $P(c)$  appears to be a power law, with exponent  $\phi_c$  depending on the specifics of the model.

#### 4. Summary

In this article, we have described a novel class of models incorporating adaptive dynamics on a lattice of nonlinear (typically chaotic) elements. We demonstrate the wide repertoire of dynamical patterns these systems are capable of supporting. The spectrum of emergent spatio-temporal phenomena ranges from spatio-temporal fixed points and cycles, to parameter regimes marked by scaling properties, as manifest in clearly defined  $1/f$  spectral characteristics and power law distributions of spatial quantities. The capacity of these models to yield wide ranging dynamical patterns by tuning just one parameter,

underscores their utility as versatile paradigms of spatio-temporal complexity in extended systems.

### References

- [1] J Crutchfield and K Kaneko, in *Directions in chaos* edited by Hao Bai-Lin (World Scientific, Singapore, 1987) and references therein
- [2] B B Mandelbrot, *Fractal geometry of nature* (Freeman, San Francisco, 1982)  
T Vicsek, *Fractal growth phenomena* (World Scientific, Singapore, 1989)
- [3] W H Press, *Comm. Mod. Phys.* **C7**, 103 (1978)
- [4] S Sinha and D Biswas, *Phys. Rev. Lett.* **71**, 2010 (1993)  
S Sinha, *Int. J. Mod. Phys.* **B9**, 875 (1995)
- [5] S Sinha, *Phys. Rev.* **E49**, 4832 (1994)
- [6] K Kaneko, *Physica* **D54**, 5 (1991) and references therein
- [7] S Sinha, *Phys. Lett.* **A199**, 365 (1995)
- [8] P Bak, C Tang and K Wiesenfeld, *Phys. Rev. Lett.* **59**, 381 (1987); *Phys. Rev.* **A38**, 364 (1988)
- [9] R Kapral, *J. Math. Chem.* **6**, 113 (1991) and references therein
- [10] B Huberman and E Lumer, *IEEE Trans. Circuits and Systems* **37**, 547 (1990)  
S Sinha, R Ramaswamy and J Subba Rao, *Physica* **D43**, 118 (1990) and references therein
- [11] Note that the probabilities reported throughout ( $P(c)$ ,  $P(s)$  and  $P(k)$ ) are in arbitrary units, and are not normalized to unity. Of course, this does not affect any of the conclusions reached by inspecting the graphs